Chinese Chemical Letters 35 (2024) 108763

Contents lists available at ScienceDirect

Chinese Chemical Letters

journal homepage: www.elsevier.com/locate/cclet

Facile synthesis of high-brightness green-emitting carbon dots with narrow bandwidth towards backlight display

Rui Cheng*, Tingting Zhang, Xin Huang, Jian Yu*

State Key Laboratory of Materials-Oriented Chemical Engineering, College of Chemical Engineering, Nanjing Tech University, Nanjing 210009, China

ARTICLE INFO

Article history:
Received 6 May 2023
Revised 28 June 2023
Accepted 2 July 2023
Available online 4 July 2023

Keywords:
Carbon dots
One-step synthesis
Narrow bandwidth
High quantum yield
Display

ABSTRACT

High-performance carbon dots (CDs) allowing the application in high-end display devices are highly desirable and usually limited by the absence of simple and easy synthesis methods. In this work, we exploited an easy-to-implement strategy for the one-step synthesis of green-emitting CDs (G-CDs) with superb optical properties. The G-CDs were synthesized using *m*-phenylenediamine (*m*-PD) as a single precursor, and the reaction reacted at 180 °C for 12 h The resultant G-CDs exhibit high-purity and excitation-independent green fluorescence with the photoluminescence (PL) peak located at 516 nm, full width at half maximum (FWHM) of 46 nm, and PL quantum yield (QY) of ~80% under the 470 nm excitation light. The G-CDs and corresponding composite film prepared with polyvinyl butyral (G-CDs@PVB) exhibit good PL stability after undergoing long-time storage for one year and 360 h exposure under 460 nm blue light. The G-CDs@PVB film was used as color-conversion materials in green-emitting light-emitting diode (LED) application, exhibiting a Commission internationale de l'Eclairage (CIE) chromaticity coordinate of (0.21, 0.44). The film was also used in CD-based liquid crystal display (CD-LCD) application, achieving a color gamut value of 85%. This work will offer a working basis for the synthesis of high-performance CDs as well as their application in displays.

© 2024 Published by Elsevier B.V. on behalf of Chinese Chemical Society and Institute of Materia Medica, Chinese Academy of Medical Sciences.

Carbon dots (CDs) are regarded as the superstars of photoluminescent nanomaterials at this stage, benefiting from their interesting physicochemical and optical properties, such as wavelength-tunable emission spectra, outstanding optical stability, plentiful surface functional groups and low toxicity [1–7]. However, the wide bandwidth emission drastically reduces the color purity of CDs, overshadowing their prospect in optoelectronic display devices.

Unfortunately, there is still no simple and universal method devoted to the preparation of CDs with narrow band and bright photoluminescence (PL), but some researchers have proposed effective examples for reference. Yuan *et al.* [8] successfully prepared multicolor emissive CDs with ultra-narrow bandwidth, whose full width at half maximums (FWHM) of blue-, green-, yellow- and red-emitting CDs were 30, 29, 30 and 30 nm. This work pioneered the study of CDs with outstanding optical performance and widened the path of CDs in high-performance display devices. Liu's group developed a kind of high-performance green emissive silanized CDs accompanied by PL quantum yield (QY) of ~93% and FWHM of 38 nm [9]. The high fluorescent intensity of CDs benefited from the alleviation of the spin-orbit coupling effect. Yang *et al.* prepared red emissive CDs with an ultra-narrow FWHM of 20 nm [10]. They considered that the π conjugated system organized with nitrogen heterocyclic and aromatic rings dominates the unitary PL center, leading to the higher PL QY and narrow FWHM. Although there have been some excellent examples demonstrating the controlled preparation of high-performance CDs, these methods usually require complex purification operations such as dialysis and silica column chromatography [11–17], which are regarded as efficient methods for isolating the by-products and precursors and improving the optical characteristics of CDs [18]. Definitely, the controlled synthesis of high-performance CDs also enables the construction of CD-based displays, including electroluminescent and photoluminescent devices. Yuan *et al.* implemented the construction of multicolor CD-based light-emitting diodes (LEDs), which were regarded as the precondition for the realization of high-end displays [8]. Liu's group constructed a CD-based wide-color-gamut backlight display with green-emitting CDs and red phosphor [19]. The display device shows a color gamut that is wider than most conventional display devices, with a value of 107%. Additionally, it achieves a high luminous efficacy of 117.43 lm/W, making it an energy-efficient option for display technology. The successful application of CDs in high-end display

* Corresponding authors.
E-mail addresses: crui0309@njtech.edu.cn (R. Cheng), Yuj@njtech.edu.cn (J. Yu).

https://doi.org/10.1016/j.cclet.2023.108763
1001-8417/© 2024 Published by Elsevier B.V. on behalf of Chinese Chemical Society and Institute of Materia Medica, Chinese Academy of Medical Sciences.

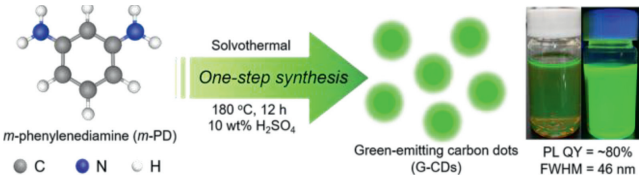

Fig. 1. Schematic diagram for one-step preparation of high-performance G-CDs.

devices will accelerate the research on the preparation methods of CDs as well as their applications.

Herein, we exploited an easy-to-implement strategy for the one-step synthesis of green-emitting CDs (G-CDs) with superb optical properties. As shown in Fig. 1, *m*-phenylenediamine (*m*-PD) was used as a single precursor, 10 wt% dilute H_2SO_4 was used as an additive and absolute ethyl alcohol was used as a solvent. The reaction reacted in an autoclave at 180 °C for 12 h and the resultant G-CDs were obtained without additional purification processes. The resultant G-CDs exhibit high-purity and excitation-independent green fluorescence accompanied by the PL peak located at 516 nm, PL QY of ~80% and FWHM of 46 nm. The G-CDs show good dispersibility in various polar solvents, endowing the potential of construction multifunctional composite film with polymers. Polyvinyl butyral (PVB) was used as a polymer matrix to construct polymer film with G-CDs (G-CDs@PVB), exhibiting good PL properties (PL peak of 520 nm, PL QY of ~76% and FWHM of 52 nm) and PL stability. In this connection, the G-CDs@PVB composite films were applied to construct green emissive LED and CD-based film for backlight display (85% National Television Standards Committee (NTSC)). This work presents a simple and easy method for synthesizing high-performance G-CDs and demonstrates the application prospects in the field of optoelectronic devices, especially backlight displays.

In this work, a simple and easy method was performed to realize the one-step preparation of high-performance G-CDs. In Fig. 1, *m*-PD, a commonly used raw material for the synthesis of CDs, was employed as a single precursor. Apart from that, 10 wt% dilute H_2SO_4 was used as an additive and ethyl alcohol was used as the solvent. After 12 h of reaction at 180 °C in the autoclave, the high-performance G-CDs were obtained. The detailed operation processes were listed in Experimental Section in Supporting information. The G-CDs solution displays bright green PL with the PL peak located at 516 nm. Unlike other methods that require complex post-purification operations, the G-CDs solution exhibited high PL QY (~80%) and narrow FWHM (46 nm), having potential for application in high-performance display devices. The results demonstrate that this method can greatly save the preparation process and time of high-performance CDs, and has the prospect of industrial application.

To investigate the structural characteristics of the G-CDs, we conducted transmission electron microscope (TEM) analysis, as shown in Fig. 2a, which demonstrates the spherical morphology and uniform size distribution of the G-CDs. The inset high-resolution TEM image in Fig. 2a shows that the G-CD has obvious lattices with a lattice spacing of 0.21 nm, which is generally considered to be the (100) plane of graphitic carbon [20,21]. The diffraction pattern of G-CD also exhibits the typical structure of graphitic carbon. The statistical analysis in Fig. S1 (Supporting information) reveals that the average diameter of the G-CDs is 2.9 nm. The atomic force microscope (AFM) image in Fig. 2b further confirms the *quasi*-spherical shape of G-CDs with an average height of approximately 3 nm. The similarity in average height and diameter between the TEM and AFM results suggests that G-CDs possess a uniform, *quasi*-spherical morphology [22]. The X-ray diffraction (XRD) pattern in Fig. 2c displays a diffraction peak centered at 22°, which can be attributed to the (002) plane of graphitic carbon [23]. We also utilized Fourier transform infrared (FT-IR) spectroscopy to

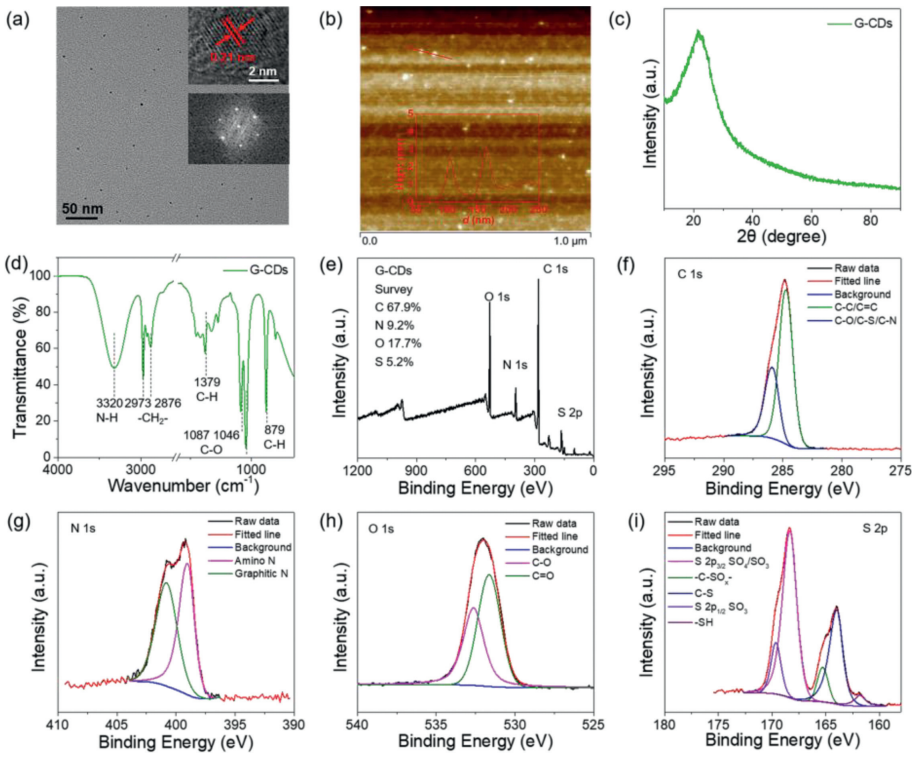

Fig. 2. (a) TEM image of G-CDs. Inset: high-resolution TEM image and diffraction pattern of a G-CD. (b) AFM image of G-CDs. Inset: height profile of the selected line in AFM image. XRD pattern (c) and FT-IR curve (d) of G-CDs. (e) XPS survey spectrum of G-CDs, and the corresponding high-resolution (f) C 1s, (g) N 1s, (h) O 1s, and (i) S 2p XPS spectra.

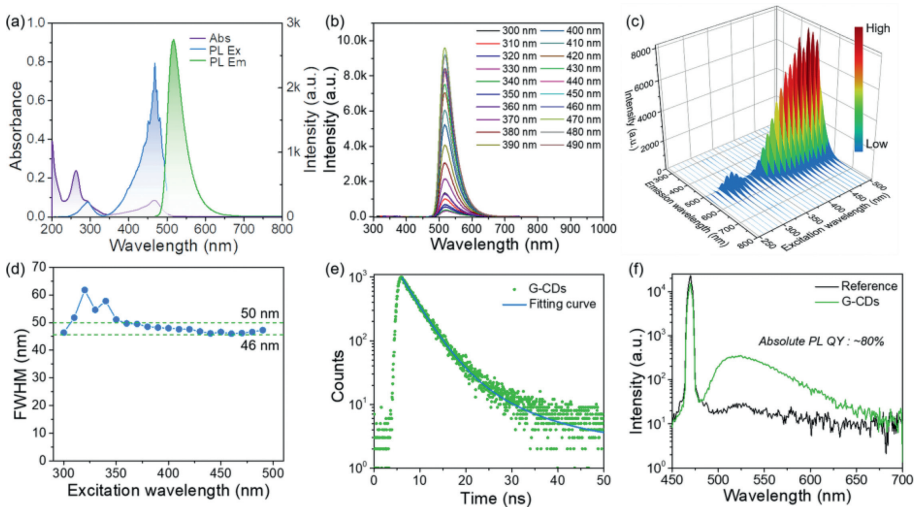

Fig. 3. (a) UV–vis absorption, PL excitation and emission spectra of G-CDs. (b) PL spectra of G-CDs under different excitation wavelengths. (c) 3D PL mapping of G-CDs under excitation wavelengths ranging from 250 nm to 490 nm with 10 nm intervals. (d) The variation of FWHM under the different excitation wavelengths. (e) The time-resolved fluorescence decay curve of G-CDs. (f) PL emission spectra used for measuring absolute PL QY. Absolute ethyl alcohol was used as a reference sample.

examine the functional groups on the surface of G-CDs, as shown in Fig. 2d. The absorption peak at 879 cm^{-1} corresponds to the out-of-plane bending vibration of C–H originating from the benzene ring of *m*-PD [24], while the absorption peaks at 1046 and 1087 cm^{-1} are assigned to the stretching vibration of C–O [25]. Additionally, the absorption peak at 1379 cm^{-1} corresponds to the C–H vibration of the sp^3 carbon [26], and the peaks at 2876 and 2973 cm^{-1} indicate the presence of methylene ($-CH_2-$) on the surface of G-CDs [27]. The absorption peak at 3320 cm^{-1} is assigned to the stretching vibration of N–H in *m*-PD [28]. To further explore the composition of G-CDs, we conducted X-ray photoelectron spectroscopy (XPS) measurements. The survey XPS spectrum in Fig. 2e indicates that the G-CDs contain C, N, O and S elements, with atomic concentrations of 67.9%, 9.2%, 17.7% and 5.2%, respectively. The C 1s spectrum in Fig. 2f confirms that the C element forms multifarious chemically bound states, including C–C/C=C (284.7 eV) [29] and C–O/C–S/C–N (285.9 eV) [30]. The N 1s spectrum shown in Fig. 2g can be divided into two peaks at 399 and 400.7 eV, which correspond to amino N and graphitic N, respectively [31,32]. The O 1s XPS spectrum in Fig. 2h exhibits two peaks, attributed to C=O (531.4 eV) [33] and C–O (532.6 eV) [34]. Finally, the S 2p XPS spectrum in Fig. 2i exhibits the existence of -SH (161.8 eV) [35], S $2p_{1/2}$ C–S (163.9 eV) [36], $-C-SO_x-$ (165.3 eV) [37], S $2p_{3/2}$ SO_4/SO_3 (168.3 eV) [38] and S $2p_{1/2}$ SO_3 (169.6 eV) [39].

The optical characteristics of the prepared G-CDs were explored. As shown in Fig. 3a, the ultraviolet–visible (UV–vis) absorption spectrum exhibits a strong peak at 263 nm and a smaller peak at 468 nm, attributed to the π-π^* transition of C=C and the *n*-π^* transition of nitrogen groups on the surface of G-CDs, respectively [40,41]. The PL emission spectrum of G-CDs shows a narrow and intense peak located at 517 nm, with a narrow FWHM of 46 nm, when excited at 460 nm, the wavelength commonly used in photoluminescent devices. The PL excitation spectrum presents two peaks centered at 293 and 468 nm. Fig. 3b demonstrates the excitation-independent behavior of G-CDs, which exhibit a consistent PL peak at 517 nm across a range of excitation wavelengths measured at 10 nm intervals between 300 nm and 490 nm. This unique property is attributed to the sulfur-doping, which suppresses the oxygen-states and enhances the nitrogen-states [42]. 3D mapping of PL spectra corresponding to Fig. 3b shows more clearly the change of PL intensity of G-CDs under various excitation lights (Fig. 3c). The overall trend of PL intensity is consistent with the PL excitation spectrum, and the variation of PL intensity at emissive peak at 517 nm was exhibited in Fig. S2 (Supporting information). In view of the fact that the mainstream fluorescent materials used for liquid crystal displays (LCDs) have the characteristics of FWHM less than 50 nm, we chose 50 nm as a benchmark condition to evaluate the FWHM of G-CDs [19]. Fig. 3d illustrates the dependence of FWHM on excitation wavelengths. The FWHMs of the PL spectra of G-CDs are below 50 nm and reach a minimum of 46 nm when excited with 470 nm light, over an optimal excitation wavelength range of 350–490 nm that covers the ultraviolet and blue light regions commonly used for excitation. The addition of dilute H_2SO_4 is believed to contribute to the narrower FWHM of G-CDs. Dilute H_2SO_4 enhances the degree of graphitization while reducing the presence of oxygen-included functional groups. As a result, the wavefunctions become more delocalized, and the bandgap fluctuation become smaller simultaneously [43]. Ultimately, these factors contribute to the observed decrease in FWHM for G-CDs. These results provide a reliable basis for the multifunctional applications of G-CDs. The fluorescence lifetime of G-CDs was obtained by fitting the time-resolved fluorescence decay curve using a bi-exponential decay function, and the fluorescence lifetime was found to be 4.76 ns (Fig. 3e). The absolute photoluminescence quantum yield (PL QY) of G-CDs was determined using a fluorescence spectrophotometer, with absolute ethyl alcohol used as reference sample. The absolute PL QY of G-CDs is approximately 80% at the excitation wavelength of 470 nm (Fig. 3f). The results indicate that the performance of G-CDs is generally superior to that of many high-performance green-emitting CDs that have a PL QY of 50% or more (Table S1 in Supporting information). The high PL QY of G-CDs may originate from the high N-doping, attributing to the amino in *m*-PD [42]. The PL properties of purified G-CDs were also measured. Fig. S3 (Supporting information) exhibits the PL properties of purified G-CDs by dialysis and column chromatography, which shows nearly equivalent PL performance, including PL peak of 517 nm, FWHM of 47 nm, absolute PL QY of 82%. This shows that the as-prepared G-CDs contain fewer impurities and therefore have excellent PL properties. Furthermore, we thoroughly investigated the effects of different reaction parameters on the fluorescence of G-CDs. Fig. S4 (Supporting information) shows the impact of varying the volumes of 10 wt% dilute H_2SO_4 on the PL of G-CDs, revealing that the PL intensity of G-CDs is highest when the volume of 10 wt% dilute H_2SO_4 is 2 mL (Fig. S4a). Fig. S4b shows the variation in intensity and wavelength of PL peak, indicating that when the volumes of 10 wt% dilute H_2SO_4

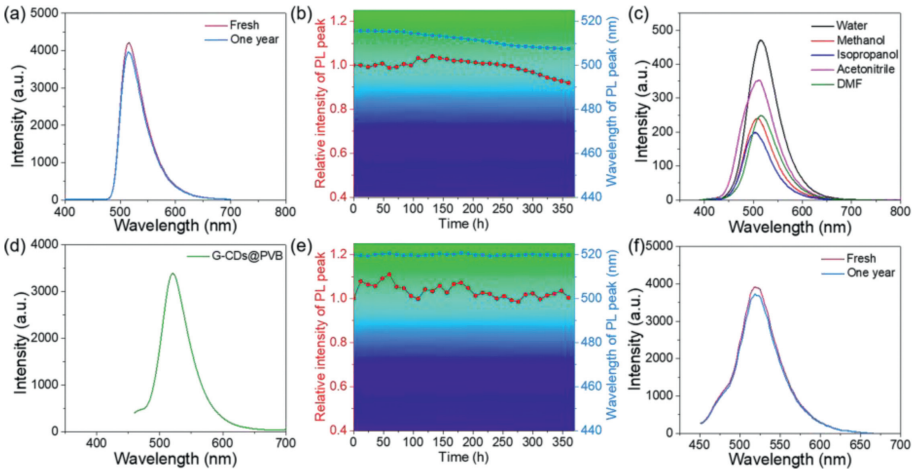

Fig. 4. (a) Comparison of PL spectra of G-CDs after one year of storage. (b) The variation of PL intensity and wavelength of G-CDs under 460 nm blue light radiation. (c) PL spectra of G-CDs in various solvents. (d) PL spectra of G-CDs@PVB film. (e) The variation of PL intensity and wavelength of G-CDs@PVB film under 460 nm blue light radiation. (f) Comparison of PL spectra of G-CDs@PVB film after one year of storage.

are more than 1 mL, the wavelength of PL peak is located in the pure green light region. Fig. S5 (Supporting information) shows the effect of varying the mass concentration of H_2SO_4 on the PL of G-CDs, with the optimal mass concentration of H_2SO_4 found to be 10%. Finally, Figs. S6 and S7 (Supporting information) exhibit the variation in intensity and wavelength of PL peak with different reaction temperatures and times, with the optimum reaction temperature and time found to be 180 °C and 12 h, respectively. Among many experimental parameters, the introduction of dilute sulfuric acid is the main factor affecting the PL properties of G-CDs. In addition to promoting the degree of graphitization and reducing the presence of oxygen-included functional groups, dilute H_2SO_4 promotes the edge amino protonation, which is also an important reason for improving the PL properties of G-CDs [11]. Fig. S8 (Supporting information) exhibits the PL spectra of G-CDs at different pH values. It can be seen that with the increase of pH values, the PL intensities of G-CDs gradually decrease, the FWHMs also increased from 46 nm to 68 nm. It is proved that edge amino protonation by dilute H_2SO_4 is the main factor to improve the PL properties of G-CDs. As the isomers of *m*-PD, *o*-phenylenediamine (*o*-PD) and *p*-phenylenediamine (*p*-PD) are usually used to synthesis of high-performance CDs. In this work, *o*-PD and *p*-PD were served as precursors to prepare CDs with the same method. Fig. S9 (Supporting information) exhibits the PL spectra of CDs prepared with *o*-PD and *p*-PD, showing relatively poor PL properties, such as extremely low PL intensities and wide FWHMs. This phenomenon confirmed that the preparation method is only applicable to *m*-PD.

The potential application of G-CDs was assessed by investigating their PL stability. In Fig. 4a, the PL spectrum of G-CDs remained unchanged after one year of storage, with the PL peak at 517 nm and 94% of the initial PL intensity maintained. Given that G-CDs are often exposed to long periods of blue light radiation during use, their stability under blue light irradiation was investigated. Fig. 4b shows that after 360 h of blue light radiation at 460 nm, the PL peak wavelength of G-CDs decreased gradually from 517 nm to 509 nm, but still remained in the green light region. Moreover, the PL intensity was maintained at 92% of the initial value. The G-CDs exhibit excellent dispersibility in various polar solvents, and also emit bright green fluorescence (Fig. S10 in Supporting information). The dispersibility of G-CDs in different solvents implies the potential to prepare diverse composites. The G-CDs@PVB film, which exhibited superior film-forming and optical properties, was also investigated (Fig. S11 in Supporting information). Fig. 4d shows that the PL spectrum of G-CDs@PVB film had a PL peak at 520 nm, a narrow FWHM of 52 nm, and a PL QY of ~76%. The PL intensity and wavelength of the G-CDs@PVB film remained almost constant after 360 h of blue light radiation, as shown in Fig. 4e, and the PL peak and intensity remained unchanged after one year of storage, as shown in Fig. 4f.

The good optical characteristics of G-CDs@PVB film endow it with the potential for applications in optoelectronic devices. LED is a common light-emitting device that G-CDs@PVB film can serve as light-conversion material to construct green-emitting LED [44]. In this work, a GaN chip with an emissive wavelength of 440 nm was used as excitation light source and green-emitting G-CDs@PVB film was pasted on the chip to convert blue light into green light. The digital photograph of the lighted green-emitting LED is shown in Fig. S12a (Supporting information), exhibiting bright green light. Fig. S12b (Supporting information) presents the luminescence spectrum of green-emitting LED. The spectrum shows two PL peaks located at 440 and 520 nm, attributing to blue GaN chip and G-CDs@PVB film, respectively. The FWHM of the green light spectrum still maintains ~52 nm, confirming the good PL stability of G-CDs@PVB film in LED devices. The Commission internationale de l'Eclairage (CIE) chromaticity coordinate for the green-emitting LED is (0.21, 0.44), which is located in the green light region (Fig. S12c in Supporting information).

The G-CDs@PVB film has a good film-forming property, having the intrinsic potential to produce large-area films by a scratch coating method. Large-area films are suitable for use as light-conversion film to construct backlight display. In this work, G-CDs were employed as light-conversion material to construct CDs based liquid crystal display (CD-LCD). Fig. 5a exhibits the simplified structure diagram of backlight units in an LCD: blue light chips and the corresponding optical films make up the blue light source; green-emitting G-CDs@PVB film and red-emitting $K_2SiF_6:Mn^{4+}$ (KSF) film are employed as green and red light conversion films. The detailed luminous and imaging principles were introduced in our previous work [45–48]. Fig. 5b shows the digital photograph of G-CDs@PVB film prepared by scratch coating method with the size of 14 × 20 cm. The G-CDs@PVB film under daylight presents a faint yellow and translucent character, facilitating the excitation and compounding of light [45]. Fig. 5c displays the digital photograph of G-CDs@PVB film taken under 365 nm UV light to prove its good optical property and its ability to be used as green light-conversion film to construct backlight displays. Fig. 5d shows the imaging effect of the resultant CD-LCD device, displaying the saturated green and red light at leaves and flowers

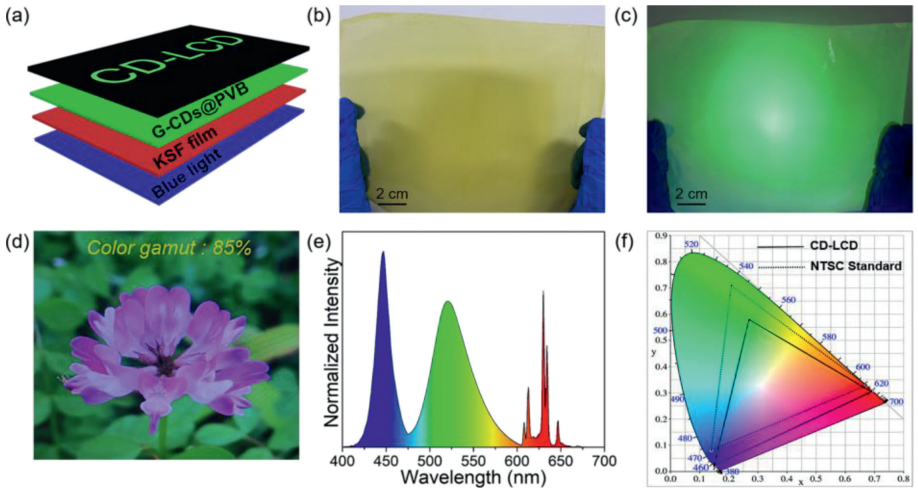

Fig. 5. (a) The simplified structure diagram of backlight units in LCD. The digital photograph of G-CDs@PVB film taken under (b) daylight and (c) 365 nm UV light. (d) The imaging effect of the resultant CD-LCD device with green-emitting G-CDs@PVB film and red-emitting KSF film. (e) The luminescent spectrum of CD-LCD. (f) The color gamut comparison between CD-LCD and NTSC standard. Solid black line: the color gamut of CD-LCD. Black dotted line: the color gamut of NTSC standard.

on the screen. The imaging effect of semi-finished LCD without color-conversion films is shown in Fig. S13 (Supporting information), demonstrating the significant improvement of display effect compared to CD-LCD. Fig. 5e displays the luminescent spectrum of CD-LCD, which presents three peaks located at 450, 520 and 630 nm, attributing to the light of blue light chips, G-CDs@PVB film and KSF film, respectively. Fig. 5f shows the color gamut comparison with NTSC standard, to give a satisfactory color gamut value of 85%, which falls within the relatively moderate range for CDs-based displays (Table S2 in Supporting information) but still exceeds that of the majority of commercial display devices [49].

In this work, we exploited an easy-to-implement strategy for the one-step preparation of green-emitting CDs with high PL QY and narrow FWHM. This method avoids complex and time-consuming processes of purification, having the advantage of greater cost reduction and high efficiency in commercialization. The resultant G-CDs stock solution exhibits excitation-independent green fluorescence with PL peak centered at 517 nm with a narrow FWHM of 46 nm and PL QY of ~80% under the excitation light of 470 nm. Additionally, the G-CDs possess good PL stability in long-time storage for one year and 360 h exposure under 460 nm blue light, still maintaining 94% and 92% of the initial PL intensity, respectively. The plentiful surface functional groups endow G-CDs with excellent dispersibility in various polar solvents, having the potential of constructing multifunctional composite films with polymers. The G-CDs@PVB film was prepared by directly mixing G-CDs and PVB polymer in the solvent of ethyl alcohol, showing green fluorescence with PL peak centered at 520 nm, PL QY of ~76% and FWHM of 52 nm. The green-emitting LED was constructed by pasting G-CDs@PVB film on a 440 nm GaN chip, showing green light with a CIE coordinate of (0.21, 0.44). In the end, we constructed CD-LCD with green-emitting G-CDs@PVB film and red-emitting KSF film used as color-conversion films, giving a satisfactory color gamut value of 85%, exceeding the color gamut value of conventional LCDs. This work presents the easy-to-perform method to synthesize high-performance G-CDs, opening the way for the industrial production of CDs and their commercial application in the field of display.

Declaration of competing interest

The authors declare that they have no known competing financial interests or personal relationships that could have appeared to influence the work reported in this paper.

Acknowledgments

This work was supported by the Jiangsu Funding Program for Excellent Postdoctoral Talent (No. 2022ZB369), Priority Academic Program Development of Jiangsu Higher Education Institutions (PAPD).

Supplementary materials

Supplementary material associated with this article can be found, in the online version, at doi:10.1016/j.cclet.2023.108763.

References

[1] L. Ethordevic, F. Arcudi, M. Cacioppo, et al., Nat. Nanotechnol. 17 (2022) 112–130.
[2] L. Ai, H. Liu, R. Liu, et al., Sci. China Chem. 65 (2022) 2274–2282.
[3] Y. Zhang, M. Li, S. Lu, Small 19 (2022) 2206080.
[4] L. Ai, Z. Song, M. Nie, et al., Angew. Chem. Int. Ed. 62 (2023) e202217822.
[5] J. Liu, T. Kong, H.M. Xiong, Adv. Mater. 34 (2022) 2200152.
[6] B. Wang, G.I.N. Waterhouse, S. Lu, Trends Chem. 5 (2023) 76–87.
[7] X. Yang, X. Li, B. Wang, et al., Chin. Chem. Lett. 33 (2022) 613–625.
[8] F. Yuan, T. Yuan, L. Sui, et al., Nat. Commun. 9 (2018) 2249.
[9] J. Chen, W.R. Liu, Y. Li, et al., Chem. Eng. J. 428 (2022) 131168.
[10] J. Liu, Y. Geng, D. Li, et al., Adv. Mater. 32 (2020) 1906641.
[11] Q. Zhang, R. Wang, B. Feng, et al., Nat. Commun. 12 (2021) 6856.
[12] B. Zhi, X. Yao, M. Wu, et al., Chem. Sci. 12 (2020) 2441–2455.
[13] H. Ding, S.B. Yu, J.S. Wei, et al., ACS Nano 10 (2016) 484–491.
[14] F. Shan, L. Fu, X. Chen, et al., Chin. Chem. Lett. 33 (2022) 2942–2948.
[15] B. Wang, Z. Wei, L. Sui, et al., Light-Sci. Appl. 11 (2022) 172.
[16] C. Wei, S. Hu, F. Liang, et al., Chin. Chem. Lett. 33 (2022) 4116–4120.
[17] H. Ren, Y. Yuan, A. Labidi, et al., Chin. Chem. Lett. 34 (2023) 107998.
[18] J. Guo, Y. Lu, A.Q. Xie, et al., Adv. Funct. Mater. 32 (2022) 2110393.
[19] J. Chen, X. Zou, W. Li, et al., Adv. Opt. Mater. 10 (2022) 2200851.
[20] M. Han, S. Lu, F. Qi, et al., Solar RRL 4 (2020) 1900517.
[21] S. Lu, G. Xiao, L. Sui, et al., Angew. Chem. Int. Ed. 56 (2017) 6187–6191.
[22] B. Wang, H. Song, Z. Tang, et al., Nano Res. 15 (2021) 942–949.
[23] Z. Wang, H. Liao, H. Wu, et al., Anal. Methods 7 (2015) 8911–8917.
[24] B.E. Kwak, H.J. Yoo, D.H. Kim, Adv. Opt. Mater. 7 (2019) 1900932.
[25] I. Perelshtein, N. Perkas, S. Rahimipour, et al., Nanomaterials 10 (2020) 1384.
[26] A. Basu, A. Suryawanshi, B. Kumawat, et al., Analyst 140 (2015) 1837–1841.
[27] H. Yang, Y. Liu, Z. Guo, et al., Nat. Commun. 10 (2019) 1789.
[28] K. Sato, R. Sato, Y. Iso, et al., Chem. Commun. 56 (2020) 2174–2177.
[29] S. Tao, S. Lu, Y. Geng, et al., Angew. Chem. Int. Ed. 57 (2018) 2393–2398.
[30] F. Li, Y. Li, X. Yang, et al., Angew. Chem. Int. Ed. 57 (2018) 2377–2382.
[31] X. Zhou, K. Yi, Y. Yang, et al., Nano Res. 15 (2022) 9470–9478.
[32] W.J. Wang, J. Wu, Y.X. Xing, et al., Sensor. Actuat. B: Chem. 360 (2022) 131645.
[33] S. Wu, W. Li, W. Zhou, et al., Adv. Opt. Mater. 6 (2017) 1701150.
[34] W.U. Khan, L. Qin, L. Chen, et al., Anal. Chim. Acta 1245 (2023) 340847.
[35] Z. Zhou, E.V. Ushakova, E. Liu, et al., Nanoscale 12 (2020) 10987–10993.
[36] Y. Song, H. Li, F. Lu, et al., J. Mater. Chem. B 5 (2017) 6008–6015.
[37] Y. Liu, W. Duan, W. Song, et al., ACS Appl. Mater. Interfaces 9 (2017) 12663–12672.

[38] B. Han, Y. Li, T. Peng, et al., Anal. Methods 10 (2018) 2989–2993.
[39] D.P. Narayanan, S.K. Cherikallinmel, S. Sankaran, et al., J. Colloid Interface Sci. 520 (2018) 70–80.
[40] W. Chen, J. Fan, X. Wu, et al., New J. Chem. 45 (2021) 5114–5120.
[41] C. Rodwihok, T.V. Tam, W.M. Choi, et al., Nanomaterials 12 (2022) 702.
[42] L. Ai, Y. Yang, B. Wang, et al., Sci. Bull. 66 (2021) 839–856.
[43] G.H. Oh, B.S. Kim, Y. Song, S. Kim, Appl. Surf. Sci. 605 (2022) 154690.
[44] J. Guo, Y. Chen, P. Zhang, et al., Chin. Chem. Lett. 35 (2024) 108481.
[45] R. Cheng, Z.B. Liang, L. Zhu, et al., Angew. Chem. Int. Ed. 61 (2022) e202204371.
[46] R. Cheng, K. Ma, H.G. Ye, et al., J. Mater. Chem. C 8 (2020) 6358–6363.
[47] R. Cheng, H. Shen, Z. Chen, et al., Mater. Lett. 254 (2019) 171–174.
[48] R. Cheng, F. Li, J. Zhang, et al., J. Mater. Chem. C 7 (2019) 4244–4249.
[49] Y. Zhang, J. Xiao, P. Zhuo, et al., ACS Appl. Mater. Interfaces 11 (2019) 46054–46061.